



Characterization of some alkali borate glasses using ultrasonic and spectroscopic techniques

Sumathi T.*, Parkavi S., Soundaraj C. and Jetruth Mary Alphonsa K.

Department of Physics, Annamalai University, Annamalai Nagar – 608 002, India
tsumathi92@gmail.com

Available online at: www.isca.in, www.isca.me

Received 5th December 2024, revised 30th April 2025, accepted 17th May 2025

Abstract

In this present work, different compositions of $70\text{B}_2\text{O}_3 - (30-x)\text{PbO} - x\text{K}_2\text{O}/\text{Li}_2\text{O}$ ($x = 2, 4, 6, 8, 10$) glasses were prepared by using melt quenching technique. The longitudinal and transverse ultrasonic velocities were measured at 10 MHz using the overlapped pulse echo approach at room temperature. Evaluations of various parameters such as molar volume, Poisson's ratio, acoustic impedance, microhardness, Debye temperature and thermal expansion coefficient have been calculated by using the measured values of density, velocity, and elastic constants. Changes in the glass network's structure with compositions are examined in relation to these parameter alterations. Using XRD and SEM, the amorphous nature and morphology of the glass samples are examined. The functional groups were identified in the glass samples by using the FTIR analysis.

Keywords: Melt quench, Debye temperature, acoustic impedance, microhardness, XRD, FTIR and SEM.

Introduction

There is an ever increasing interest in the measurement of elastic properties of solids using ultrasonic method due to their non-destructive nature. Elastic properties of solid materials are of considerable significance because their measurement yields information concerning the forces that operate between the atoms or ions comprising solids. This is fundamentally important in interpreting and understanding the native bonding in the solid state materials.

The choice of the most appropriate material for particular application requires knowledge of its mechanical properties. Hence, elastic properties are suitable for describing the glass structure as a function of composition¹.

The study of oxide glasses has gained attention due to their structural features. Several recent studies have been made concerning the physical properties of borate oxide glasses^{2,3}. Borate glasses, in particular, offer significant benefits such as ease of preparation and shaping, affordability, a low melting point, high transparency and sensitivity as well as superior thermal stability^{4,5}. Alkali borate glasses have been extensively studied over the years to elucidate the nature and relative concentration of various borate units constituting the glass network. Alkali metals significantly alter the network structure of borate glass, impacting its microscopic structure and physical properties based on the alkali content.

As alkali ions increase, the boron coordination number shifts from three to four, creating non-bridging oxygens. This structural change forms various groups like pentaborate,

dipentaborate, diborate, triborate and metaborate, depending on the specific alkali metal and its concentration⁶.

Structure and the physical properties of lead borate glasses have been of considerably increasing interest due to their possible potential applications in enamels, photonics and opto-electronic applications. Glasses containing divalent ions such as Mg^{2+} , Zn^{2+} , Pb^{2+} , Ca^{2+} , etc., play an important role both in the formation and modification of glass structure. Physical properties of borate glasses can be altered by the addition of a network modifier (alkali and alkaline earth oxides). Several works on alkali borate glasses have shown that there is a correlation between elastic properties and borate glass structure⁷⁻⁹.

Many investigations have been carried out to improve the properties of glasses. It has been shown that introducing alkali metal oxides, such as K_2O and CaO , is an effective way to enhance physical properties, increase chemical durability and boost moisture resistance¹⁰. Borate glasses containing Li^+ have been extensively studied due to their technological applications in solid-state batteries¹¹. Small size, light weight and high electropositive character of lithium ions are considered as factors which give rise to high energy densities. K_2O is commonly used as a glass flux to lower the working temperature and also plays a significant role in controlling thermal expansion¹². In borates, formations of groups like boroxol are illustrative of tight connectivities. The concentration of the various borate species in the glass structure is however determined by the nature and concentration of the modifier oxides. For example, addition of alkali oxides breaks not only the B-O-B bonds but also the tightly organized borate units. As

a consequence of such structural changes, properties of alkali borate glasses vary nonlinearly as a function of composition and often give rise to maxima and minima described as 'boron anomaly'.

The elastic moduli of glasses are influenced by many physical parameters, which involve the measurement of ultrasonic velocities. The elastic properties, which are inherently linked to glass structure, can be determined by measuring ultrasonic wave velocities and density. The present work aims at the preparation of following three series of glasses (one binary and two ternary systems) namely B_2O_3 -PbO, B_2O_3 -PbO- K_2O and B_2O_3 -PbO- Li_2O . Ultrasonic velocity and density measurements have been made on the glass specimen.

Materials and Methods

Two series of glasses, each containing 5 specimens, are prepared from AR grade chemicals (minimum assay 99.9%) B_2O_3 , PbO, Li_2O and K_2O . The required amount (approximately 10g) of different chemicals in powder form is weighed using a single pan digital balance having an accuracy of $\pm 0.0001g$. The homogenization of the appropriate mixture of the components of chemicals is effected by repeated grinding using a mortar. The homogeneous mixture is put in a platinum crucible and placed in a furnace. Melting is carried out under controlled conditions at a temperature from 900 to 1000°C for both systems. The molten sample is cast into a copper mould having dimensions of 10mm diameter and 6mm length. Then the glass samples are annealed at 400°C for two hours to avoid the mechanical strain developed during the quenching process. The samples prepared are chemically stable and non-hygroscopic. The prepared glass samples are polished and the surfaces are made perfectly plane and smoothed by diamond disc and diamond powder. Thickness of the samples has been measured using digital verniercalipers with an accuracy of 0.0001mm. The photographs of BPK and BPL systems are displayed in Figure-1 and 2. The nomenclature and the composition in mol % of different glass specimen are listed in Table-1.



Figure-1: BPK Glass Specimen.



Figure-2: BPL Glass Specimen.

Table-1: Nomenclature and composition of glasses.

Sample No.	Nomenclature	Composition in mol%	Remarks
Plate I	B_2O_3 -PbO- K_2O	B_2O_3 -PbO- K_2O	Mol% of B_2O_3 is constant
1	BPK2	70-28-2	
2	BPK4	70-26-4	
3	BPK6	70-24-6	
4	BPK8	70-22-8	
5	BPK10	70-20-10	
Plate II	B_2O_3 -PbO- Li_2O	B_2O_3 -PbO- Li_2O	
1	BPL2	70-28-2	
2	BPL4	70-26-4	
5	BPL10	70-20-10	

Theory and Calculations: Various parameters of the glass specimen are calculated using the measured density (ρ), longitudinal velocity (U_l) and shear velocity (U_s) using the standard expression¹³⁻¹⁵ given below:

$$\text{Measurement of Density} \quad \rho = \frac{W_A}{(W_A - W_B)} \times \rho_B \quad (1)$$

$$\text{Measurement of Velocity} \quad U = \frac{2d}{t} \quad (2)$$

$$\text{Molar volume } V_m = \frac{M}{\rho} \quad (3)$$

$$\text{Longitudinal modulus } L = \rho U_l^2 \quad (4)$$

$$\text{Shear modulus } G = \rho U_s^2 \quad (5)$$

$$\text{Bulk modulus } K = L - \left(\frac{4}{3}\right)G \quad (6)$$

$$\text{Poisson's ratio } \sigma = \left(\frac{L-2G}{2(L-G)}\right) \quad (7)$$

$$\text{Young's modulus } E = (1 + \sigma) 2G \quad (8)$$

$$\text{Acoustic impedance } Z = U \sigma \quad (9)$$

$$\text{Micro hardness } H = (1 - 2\sigma) \frac{E}{6(1+\sigma)} \quad (10)$$

$$\text{Debye temperature } \theta_D = \frac{h}{K} \left(\frac{9N}{4\pi V_m}\right)^{\frac{1}{3}} U_m \quad (11)$$

$$\text{Mean sound velocity } U_m = \left[\frac{1}{3} \left(\frac{2}{U_s^3} + \frac{1}{U_l^3} \right) \right]^{\frac{-1}{3}} \quad (12)$$

$$\text{Thermal expansion coefficient } \alpha_p = 23.2 (U - 0.57457) \quad (13)$$

Results and Discussion

The experimental values of density (ρ), longitudinal ultrasonic velocity (U_l), shear ultrasonic velocity (U_s) and molar volume (V_m) of the different glass specimen with respect to the change in the mol% of K_2O and LiO_2 used as network modifier are listed in Table-2. The calculated longitudinal modulus (L), shear modulus (G), bulk modulus (K), Young's modulus (E) and Poisson's ratio (σ) are reported in Table-3. The acoustic impedance (Z), microhardness (H), Debye temperature (θ_D) and thermal expansion coefficient are presented in Table-4.

The density is a powerful tool capable of exploring the changes in the structure of glass. The density is affected by the structural softening/compactness, change in geometrical configuration, co-ordination number, cross-link density and dimension of interstitial spaces of the glass. It is known that B_2O_3 in its glass form is a laminar network consisting of boron atoms three-fold co-ordinated with oxygen. Upon modification with an alkali oxide, the additional oxygen, obtained by the oxide dissociation causes a conversion from the trigonal boron atoms BO_3 into four-fold BO_4 co-ordinated boron atoms. Each BO_4 structural group is negatively charged and the four oxygens are included in the network as bridging oxygens. These units are responsible for the increase in the connectivity of the glass network. As a result, the degree of the structural compactness, modification of geometrical configuration etc., in the glass network can be varied with a change in the composition.

From the Table-2, the glass density decreases from 3750 to 3490 Kgm^{-3} for BPK system and 3700 to 3469 Kgm^{-3} for BPL system as the alkali modifier content (K_2O and LiO_2) increases from 0 to 10 mol%. The variations in these parameters accompanying the substitution of PbO by LiO_2 and K_2O and are related to change in the atomic mass and atomic volume of the constituent elements (lead, lithium and potassium). The atomic masses of lead, lithium and potassium atoms are 207.2u, 6.941u and 39.0983u respectively. As we increase the alkali content the density of the glasses decreases, which is probably due to the size effect with the replacement of lead atoms by the lighter potassium and lithium ions.

Table-2: Values of density (ρ), longitudinal velocity (U_l), shear velocity (U_s) and molar volume (V_m) of BPK & BPL glass systems.

Name of the Sample	Density $\rho \times 10^3 \text{ kgm}^{-3}$	Ultrasonic velocity ms^{-1}		Molar volume (V_m) cm^3/mol
		Longitudinal (U_l)	Shear (U_s)	
BP	3.8325	4453.53	2281.905	3.0187
BPK glass system				
BPK2	3.7503	4204.947	2211.896	3.0161
BPK4	3.6806	4356.364	2281.905	3.0031
BPK6	3.6206	4492.943	2332.689	2.9816
BPK8	3.5703	4583.174	2367.347	2.9514
BPK10	3.4900	4777.778	2442.191	2.9453
BPL glass system				
BPL2	3.7001	4338.235	2350.598	3.0222
BPL4	3.6530	4426.274	2386.965	2.9554
BPL6	3.6028	4568.687	2449.898	2.8892
BPL8	3.5442	4710.231	2501.062	2.8279
BPL10	3.4689	4869.105	2583.153	2.7778

Table-3: Values of longitudinal, shear, bulk and Young's Moduli and Poisson's ratio of BPK and BPL glass systems.

Name of the Sample	Longitudinal modulus $L \times 10^9 \text{Nm}^{-2}$	Shear modulus $G \times 10^9 \text{Nm}^{-2}$	Bulk modulus $K \times 10^9 \text{Nm}^{-2}$	Young's modulus $E \times 10^9 \text{Nm}^{-2}$	Poisson's ratio σ
BP	77.83	20.43	50.59	54.03	0.3220
BPK glass system					
BPK2	66.31	18.34	41.85	48.79	0.3087
BPK4	69.85	19.17	44.30	50.25	0.3109
BPK6	73.09	19.70	46.82	51.83	0.3155
BPK8	75.00	20.01	48.32	52.75	0.3181
BPK10	79.67	20.82	51.91	55.08	0.3232
BPL glass system					
BPL2	69.64	20.44	42.38	52.84	0.2922
BPL4	71.56	20.81	43.81	53.90	0.2950
BPL6	75.20	21.62	46.37	56.14	0.2982
BPL8	78.63	22.17	49.07	57.81	0.3037
BPL10	82.24	23.15	51.38	60.37	0.3042

Table-4: Values of acoustic impedance (Z), micro hardness (H), Debye temperature (θ_D) and thermal expansion coefficient (α_p) of BLC glass system.

Name of the Sample	Acoustic impedance $Z \times 10^7 \text{kgm}^{-2}\text{s}^{-1}$	Micro hardness $H \times 10^9 \text{Nm}^{-2}$	Debye temperature $\theta_D \text{K}$	Thermal expansion coefficient $\alpha_p \text{K}^{-1}$
BP	1.7477	2.4248	297.881	103308.6
BPK glass system				
BPK2	1.5770	2.3397	287.695	97541.44
BPK4	1.6034	2.4156	297.956	101054.3
BPK6	1.6267	2.4235	305.496	104222.9
BPK8	1.6363	2.4270	311.195	106316.3
BPK10	1.6674	2.4541	321.465	110831.1
BPL glass system				
BPL2	1.6052	2.8322	304.889	100633.7
BPL4	1.6167	2.8450	312.707	102676.2
BPL6	1.6460	2.9020	323.514	105980.2
BPL8	1.6694	2.9092	332.872	109264.0
BPL10	1.6890	3.0222	345.872	112949.9

Both longitudinal and shear velocities increase with increase in mol% of (K_2O and LiO_2) in both the systems but the rate of increase of U_l is greater than that of U_s . The increase in ultrasonic velocity has been attributed to an increase in packing density because of the transformation of co-ordination of boron ion. Due to this packing density, the rigidity of the glass system increases and hence the ultrasonic velocities and elastic constants^{16,11}. Poisson's ratio is defined as the ratio between lateral and longitudinal strain produced when tensile force is applied. For tensile stresses applied parallel to the chains, the produced longitudinal strain will be the same and is unaffected by the cross-link density, while lateral strain is greatly decreased with the cross-link density. This will lead to a decrease in glass rigidity¹⁷. From the Table-4, it is observed that the acoustic impedance Z increases with increase in mol% of alkali content in the glass system confirming the increase in rigidity of the

structure of the glasses. Similar trend is obtained by Raghavaraiah and Veeraiah¹⁸.

Hardness is defined qualitatively as the characteristic ability of a material to resist penetration or abrasion by other bodies. However any quantitative measure of this feature of material behaviour depends on the technique used for its measurement. It is an extrinsic property of a material rather than a fundamental or intrinsic property such as density or thermal network modifier content^{19,20}.

The amorphous nature of glass samples is confirmed by X-ray diffraction technique using an X-ray diffractometer. The glassy state of all glasses was confirmed by the absence of sharp peaks in XRD and shows no evidence of unmelted or crystalline particles in a quenched glass (Figure-3).

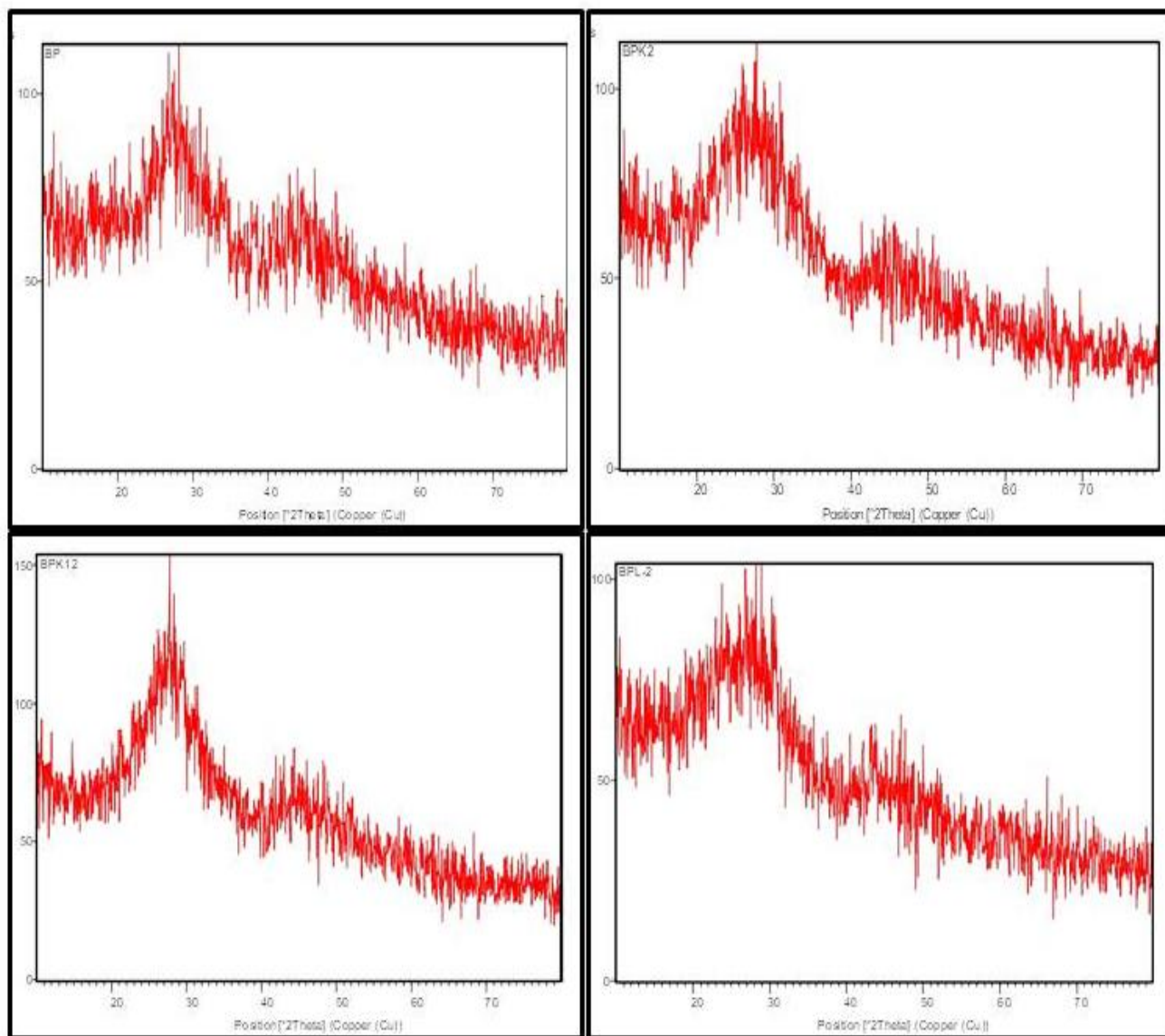


Figure-3: X-ray diffractogram of glasses BP, BPK-2, BPK-10 and BPL-2.

FTIR transmittance spectra of $70\text{B}_2\text{O}_3 - (30-x)\text{PbO} - x\text{K}_2\text{O}/\text{Li}_2\text{O}$ glasses in the frequency range between 400 and 4000cm^{-1} are shown in Figure-4. The broadening of IR bands indicated that there is no detectable change due to crystallization. The observed bands along with their vibrational assignments of samples have been tabulated in Table-5.

The vibrational modes of the borate network are active mainly in three regions. The first region lies between 600 and 800cm^{-1} and is due to bending vibration of various borate segments. ii. The second region lies between 850 and 1200cm^{-1} and is due to stretching vibrations of tetrahedral BO_4 units. The third region lies between 1200 and 1600cm^{-1} and is due to stretching vibrations of B–O in BO_3 triangles.

Borate glasses in particular, have been the subject of numerous infrared studies due to their structural peculiarities²¹⁻²³. It is generally accepted that pure boron oxide glass is built from networks of boroxol rings. B_2O_3 is one of the best and well known glass formers and is present in almost all commercially important glasses. When lead oxide is introduced to borate glasses, there are two ways in which lead ion can get incorporated into the glass, one as a modifier and the other as a former. When acting as a modifier, it behaves in the same way as alkali oxide or rare earth oxide. In this study, it disrupts the bonds connecting neighbouring BO_3 and BO_4 groups. On the

other hand, PbO can be incorporated into the glass as network forming Pb-O groups ($[\text{PbO}_4]$ and/or $[\text{PbO}_3]$).

The bands from $1346-1393\text{cm}^{-1}$ are assigned to B–O stretching vibration in $[\text{BO}_3]$ units from various types of borate groups. On passing from boron trioxide to borate glasses, a change in the coordination number of boron takes place. In these glasses, the boron is tetrahedrally surrounded by four oxygen atoms. The peak at around 1020cm^{-1} is the typical stretching vibration range of BO_4 tetrahedral from tri-, tetra- and pentaborate groups. The band has been observed in $650-720\text{cm}^{-1}$ spectral region is assigned to B–O–B bending vibrations in $[\text{BO}_3]$ triangles. Low frequency bands ($50-600\text{cm}^{-1}$) are generally attributed to vibrations of metal ions against their network sites. The band at 460cm^{-1} on the spectra of all series of glasses is attributed to the bending vibrations of the tetrahedral PbO_4 . The well-known characteristic band (at 806cm^{-1}) of vitreous B_2O_3 is assigned to the symmetric stretching vibration of the boroxol ring. The spectra show non-existence of band at 806cm^{-1} reveals the absence of boroxol rings in the glasses and hence it consists of only BO_3 and BO_4 groups. In addition to the above features, a transmittance band appears in the spectra of all glasses around 3500cm^{-1} . Such a band is attributed to stretching vibration of –OH ion. In glass structure, Pb^{2+} cations play the role of network modifier when these cations are ionically bonded. On the other hand if Pb–O band is covalent, Pb^{2+} cations will act as glass former. Similar conclusion was drawn by Motke et al.²⁴.

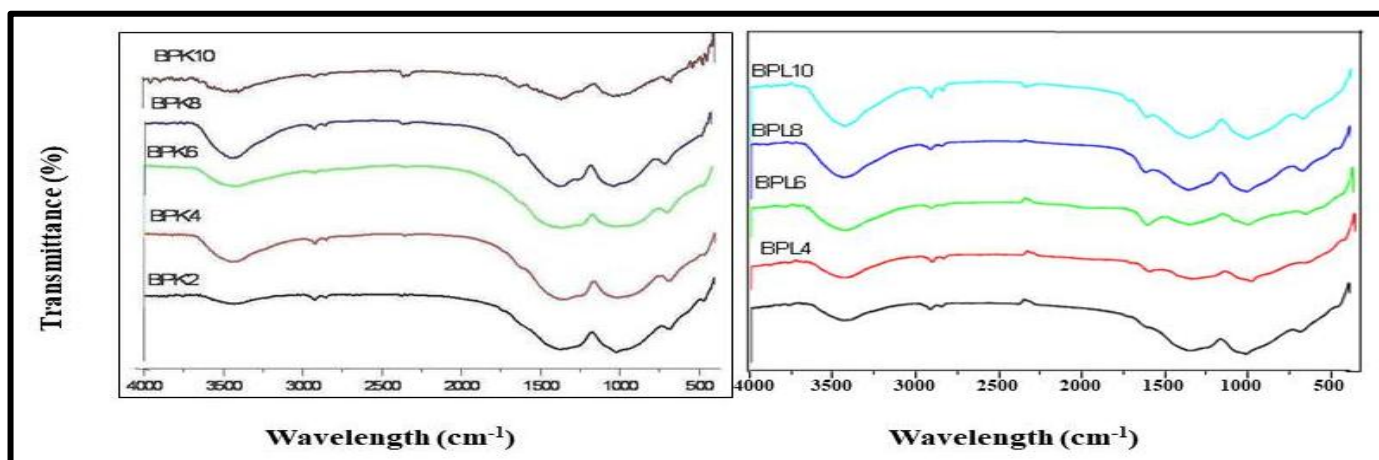


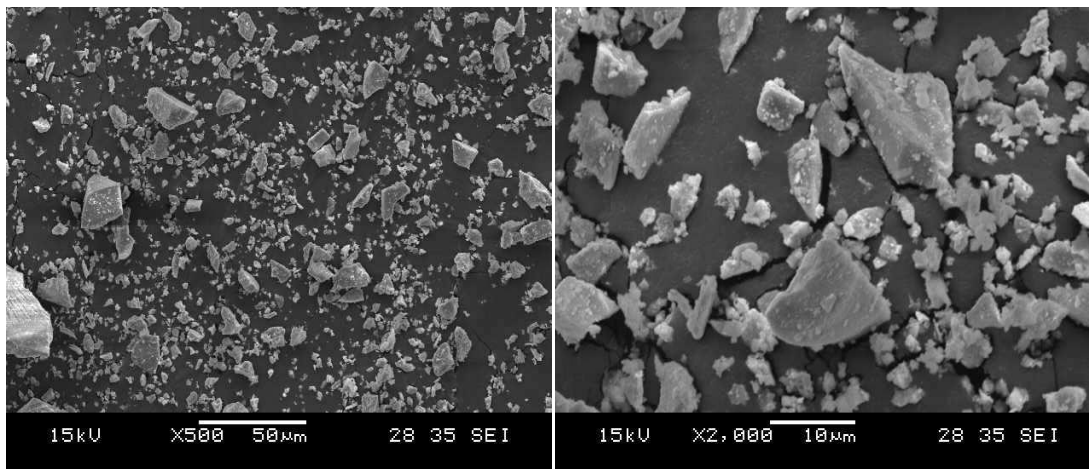
Figure-4: FTIR spectra of BPK and BPL glass specimens.

Table-5: FTIR tentative frequency assignment of BPK and BPL Glasses.

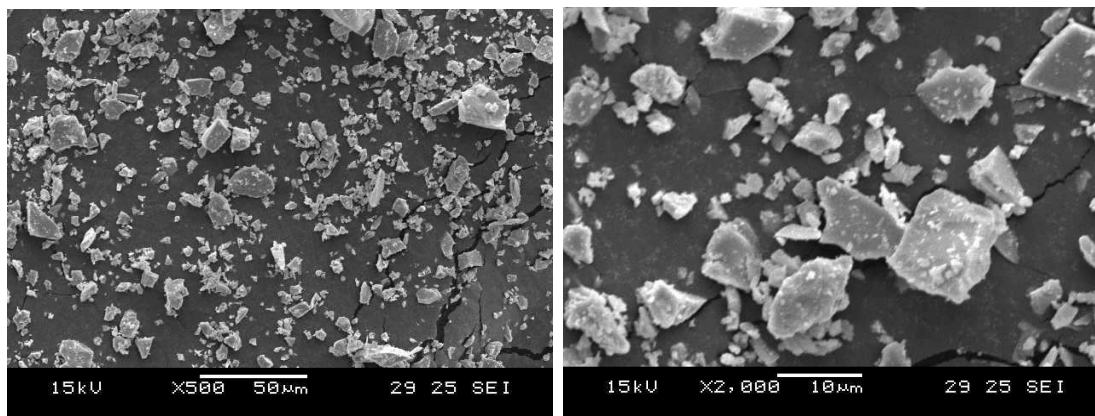
S. No.	Wave number (cm^{-1})	Band assignments	References
1	1346-1393	Stretching vibrations of B–O of trigonal $(\text{BO}_3)^{3-}$ units	25
2	1000-1100	Symmetric stretching vibrations of BO_4 units	25
3	650-720	B–O–B bending vibrations in $[\text{BO}_3]$ triangles	26
4	460	Bending vibrations of tetrahedral $[\text{PbO}_4]$	26

The morphology of the BPK and BPL glasses has been studied using SEM (JEOL Autofine coater Model JFS-1608). The SEM microphotographs of the prepared glass specimen are given in Figure-5. They suggest an idea about the shape and size of the

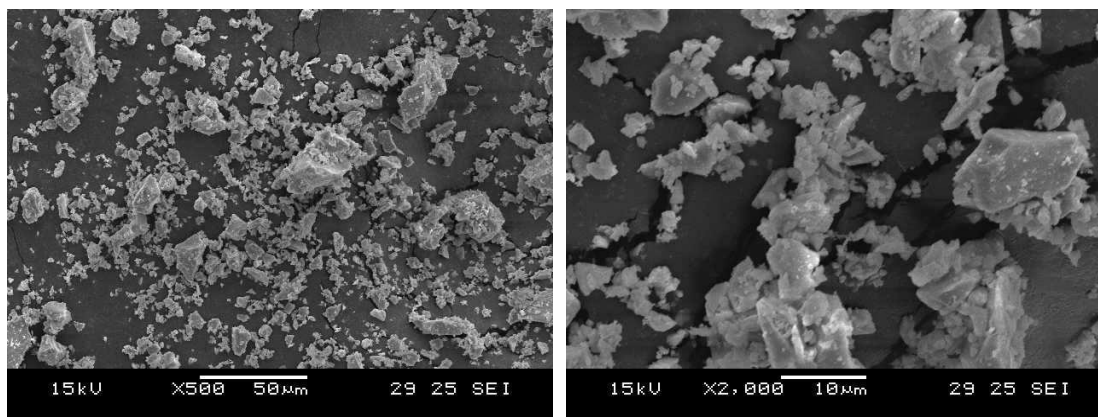
particles and the nature of the specimen. From the Figure-5, it is observed that different sized grain particles are distributed. The particle size seems to vary in each micrograph. The particles are extremely angular in nature.



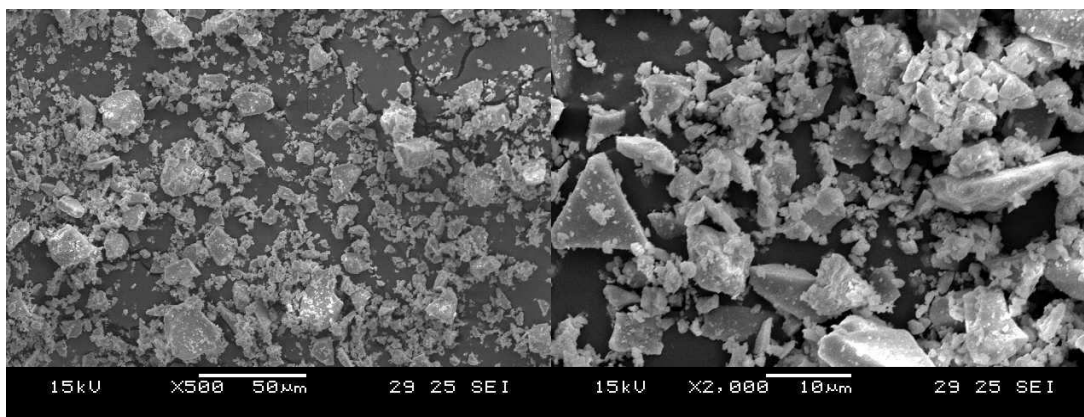
(a) BP.



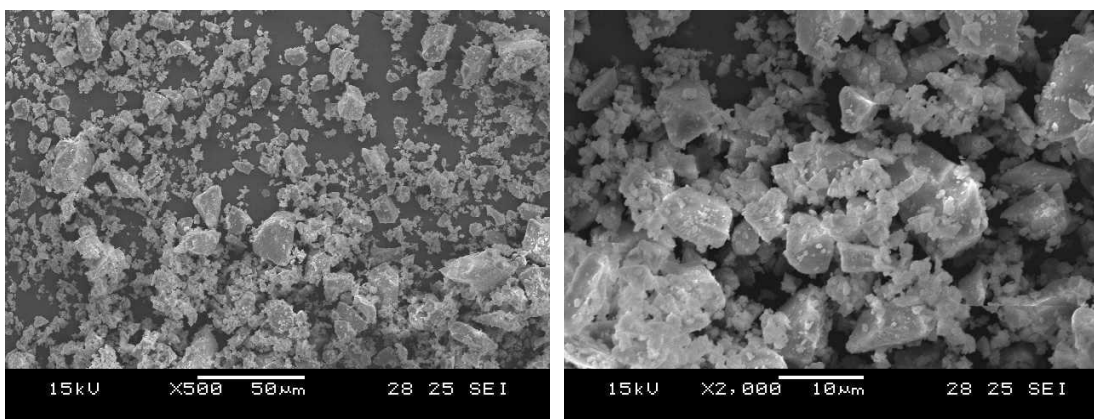
(b) BPK 2.



(c) BPK10.



(d) BPL2.



(e) BPL10.

Figure-5(a-e): SEM Photographs of alkali borate glass specimen.

Conclusion

XRD patterns predict the nature of samples is amorphous. The gradual decrease in density with mol% of K_2O and Li_2O of the glass specimen indicates the dependence of density on weight of the metal atom in the network modifier (NWM). The ultrasonic velocities (both longitudinal and shear) of both the systems vary linearly and the magnitude is in the order $BPL > BPK$. The estimated elastic moduli, acoustical and mechanical properties of the glasses throw light on the rigidity and compactness in structural network. The functional groups present in the glass samples have been confirmed by FTIR spectral analysis. The topographical aspects of the glass samples are reported from SEM micrographs.

References

1. Gowda, V. V., & Anavekar, R. V. (2004). Elastic properties and spectroscopic studies of $Na_2O-ZnO-B_2O_3$ glass system. *Bulletin of Materials Science*, 27(2), 199-205.
2. Saddeek, Y. B. (2011). Study of elastic moduli of lithium borobismuthate glasses using ultrasonic technique. *Journal of non-crystalline solids*, 357(15), 2920-2925.
3. Doweidar, H. and Yasser B. Saddeek. (2010). Effect of La_2O_3 on the structure of lead borate glasses. *J. Non. Cryst. Sol.*, 356 (28-30), 1452-1457, <https://doi.org/10.1016/j.jnoncrsol.2010.04.036>.
4. Samir, A., Hassan, M.A., Abokhadra, A., Soliman, L.I. and Elokr, M. (2019). Characterization of borate glasses doped with copper oxide for optical application. *Opt. Quant. Electron.*, 51(123), 1-13. <https://doi.org/10.1007/s11082-019-1819-7>.
5. Naik, J., Bhajantri, R.F., Hebbar, V. and Rathod, S. G. (2018). Influence of ZrO_2 filler on physicochemical properties of PVA/ $NaClO_4$ polymer composite electrolytes. *Adv. Compos. Hybrid Mater.* 1, 518-529, <https://doi.org/10.1007/s42114-018-0030-9>.
6. Seiji Kojima (2020). Mixed-Alkali Effect in Borate Glasses: Thermal, Elastic, and Vibrational Properties. *Solids*, 1(1), 16-30, <https://doi.org/10.3390/solids1010003>.
7. Mitsuru Kawashima, Yu Matsuda and Seiji Kojima (2011). Temperature dependence of elastic properties in alkali borate binary glasses. *J. Mol. Struct.*, 993(1-3), 155-159. <https://doi.org/10.1016/j.molstruc.2010.11.006>.

8. Yasser B. Saddeek. (2004). Structural analysis of alkali borate glasses. *Physica B: Condensed Matter*, 344(1-4), 163–175. <https://doi.org/10.1016/j.physb.2003.09.254>.
9. Yasser B. Saddeek (2004). Ultrasonic study and physical properties of some borate glasses. *Materials Chemistry and Physics* 83(2-3), 222–228. <https://doi.org/10.1016/j.matchemphys.2003.09.051>.
10. Matori K.A., Sayyed M.I., Sidek H.A.A., Zaid M.H.M. and Singh V.P. (2017). Comprehensive study on physical, elastic and shielding properties of lead zinc phosphate glasses. *Journal of Non-Crystalline Solids*, 457, 97-103, DOI:10.1016/j.jnoncrysol.2016.11.029., 457, 97-103.
11. Narayana Reddy C. and Sreekanth Chakradhar R. P. (2007). Elastic properties and spectroscopic studies of fast ion conducting $\text{Li}_2\text{O}-\text{ZnO}-\text{B}_2\text{O}_3$ glass system. *Materials Research Bulletin* 42(7). 1337–1347, <https://doi.org/10.1016/j.materresbull.2006.10.001>.
12. Alaoui Y., El Moudane M., Er-rafai A., Khachani M., Ghanimi A., Sabbar A., Tabyaoui M., Guenbour A., and Bellaouchou A. (2021). Structural study, thermal and physical properties of $\text{K}_2\text{O}-\text{CaO}-\text{P}_2\text{O}_5$ phosphate glasses. *Moroccan Journal of Chemistry* 454-463, DOI:10.48317/IMIST.PRSM/morjchem-v9i2.22505.
13. Asha Rani, Rajesh Parmar and Kundu R.S. (2023). Structural, physical and optical study of calcium modified bismuth borovanadate glasses: $\text{V}_2\text{O}_5-\text{B}_2\text{O}_3-\text{Bi}_2\text{O}_3-\text{CaO}$. *Optical materials* 143, 114-135, <https://doi.org/10.1016/j.optmat.2023.114135>.
14. Sumathi, T. and Kannappan, A.N., (2012). Ultrasonic Investigation on Sodium and Calcium Tungsten Phosphate Glass System. *Research journal of Chemical science* 2(9), 14-17.
15. Papadakis E. P. (1967). Ultrasonic Phase Velocity by the Pulse-Echo-Overlap Method Incorporating Diffraction Phase Corrections. *J. Acoust. Amer.*, 42, 1045-1051, <https://doi.org/10.1121/1.1910688>.
16. Narayana Reddy C. and Anavekar R.V. (2008). Elastic properties and spectroscopic studies of $\text{Li}_2\text{O}-\text{B}_2\text{O}_3-\text{V}_2\text{O}_5$ glasses. *Materials Chemistry and Physics*, 112(2), 359-365. <https://doi.org/10.1016/j.matchemphys.2008.05.062>.
17. Sidkey M. A. and Gaafar M. S. (2004). Ultrasonic studies on network structure of ternary $\text{TeO}_2-\text{WO}_3-\text{K}_2\text{O}$ glass system. *Physica B: Condensed Matter*, 348(1-4), 46-55, <https://doi.org/10.1016/j.physb.2003.11.005>.
18. Raghavariah B.V. and Veeraiah N. (2004). The role of As_2O_3 on the stability and some physical properties of $\text{PbO}-\text{Sb}_2\text{O}_3$ glasses. *J. Phys. & Chem. Sol.*, 65(6), 1153 – 1164. <https://doi.org/10.1016/j.jpcs.2004.01.004>.
19. Gaafar M.S., Abd El-Aal N.S., Gerges O.W. and El-Amir G. (2009). Elastic properties and structural studies on some zinc-borate glasses derived from ultrasonic, FT-IR and X-ray techniques. *J. Alloys Compd.*, 475(1-2), 535–542. <https://doi.org/10.1016/j.jallcom.2008.07.114>.
20. Gaafar M.S., Saddeek Y.B. and Abd-El-Latif L. (2009). Ultrasonic studies on alkali borate tungstate glasses. *J. Phys. Chem. Solids*, 7 (1), 173-179, <https://doi.org/10.1016/j.jpcs.2008.09.023>.
21. Doweidar H. and Yasser B. Saddeek (2009). FTIR and ultrasonic investigations on modified bismuth borate glasses. *J. Non. Cryst. Sol.*, 355(6), 348 – 354. <https://doi.org/10.1016/j.jnoncrysol.2008.12.008>.
22. Sherief M. Abd-Naf (2012). FTIR and UV-Vis optical absorption spectra of gammairradiated MoO_3 -doped lead borate glasses. *Journal of Non-cystalline solids*, 358(2), 406-413, <https://doi.org/10.1016/j.jnoncrysol.2011.10.013>.
23. Joao Coelho, Cristina Freire and Sooraj Hussain N. (2012). Structural studies of lead lithium borate glasses doped with silver oxide. *Spectrochim. Acta, Part*, 86, 392-398, <https://doi.org/10.1016/j.saa.2011.10.054>.
24. Motke S. G., Yawale S. P. and Yawale S. S. (2002). Infrared spectra of zinc doped lead borate glasses. *Bull. Mater. Sci*, 25, 75-78. <https://doi.org/10.1007/BF02704599>.
25. Saudi H.A., Mostafa A.G., Sheta N., El Kameesy S.U. and Sallam H.A. (2011). The structural properties of $\text{CdO}-\text{Bi}_2\text{O}_3$ -borophosphate glass system containing Fe_2O_3 and its role in attenuating neutrons and gamma rays. *Physica B*, 406 (21), 4001-4006. <https://doi.org/10.1016/j.physb.2011.06.038>.
26. Rada S., Culea M., Neumann M. and Culea E. (2008). Structural role of europium ions in lead- borate glasses inferred from spectroscopic and DFT studies. *Chemical Physics letters*, 460(1-3), 196-199, <https://doi.org/10.1016/j.cplett.2008.05.088>.